# CuInSe2 (CIS) Thin Films Prepared from Amorphous Cu−In−Se Nanoparticle Precursors for Solar Cell Application

SeJin Ahn, Kyunhwan Kim, Ara Cho, Jihye Gwak, Jae Ho Yun, Keeshik Shin, SeoungKyu Ahn, and Kyunghoon Yoon*

Solar Energy Department, Korea Institute of Energy Research, 71-2 JangDong, YuseongGu, DaeJeon, 305-343, Korea

ABSTRACT: CuInSe2 (CIS) absorber layers for thin film solar cells were formed via a nonvacuum route using nanoparticle precursors. A low-temperature colloidal process was used to prepare nanoparticles by which amorphous Cu−In−Se nanoparticles were formed within 1 min of reaction without any external heating. Raman spectra of the particles revealed that they were presumably mixtures of amorphous Cu−Se and In−Se binaries. Selenization of the precursor film prepared by doctor blade coating of the Cu−In−Se nanoparticles resulted in a facile growth of the particles up to micrometer scale. However, it also left large voids in the final film, which acted as short circuiting paths in completed solar cells. To solve this problem, we applied a solution-filling treatment in which a solution containing Cu and In ions was additionally coated onto the precoated nanoparticles, resulting in a complete infiltration of the filler solution into the pores in the nanoparticles based film. By this approach, short circuiting of the device was significantly mitigated and a conversion efficiency of up to 1.98% was obtained.

KEYWORDS: solar cell, CIS, nanoparticle, solution filling
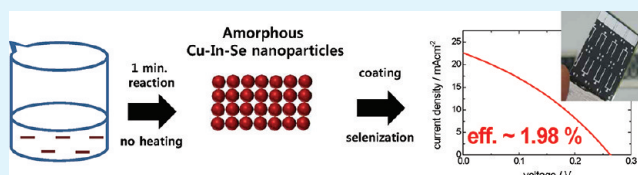
INTRODUCTION

CuInSe2 (CIS)-based chalcopyrite compounds are attracting considerable interests as light-absorbing materials for thin film solar cells on account of their inherent advantages of high absorption coefficient, adjustable bandgap and high stability under high energy irradiation. The potential of these compound semiconductors was well demonstrated by the record power conversion efficiency over 20% for the devices fabricated with CuInGaSe2 (CIGS) type thin films.[1,2]

However, in spite of the high efficiency of state-of-the-art CIGS thin film solar cells, the high production cost of the conventional vacuum-based processes such as a multi stage coevaporation and a two-step process of sputtering and selenization is considered to be a main obstacle to the widespread use of CIGS solar cells.[3]

In this regard, fabrication of CIS thin films using nanoparticle based inks is one of the most promising alternative approaches to reduce the total production costs. Advantages of CIS nanoparticle based approach include a dispersibility of the particles in organic solvents for nonvacuum coating,[4] and a relatively easy composition control of the final thin films.[5] The latter is based on the previous papers reporting that composition of the precursor nanoparticles was transferred directly to that of as-coated[6] and selenized films.[7]

Various approaches have been employed to prepare CIS-type nanomaterials including solvothermal routes,[8−11] hot injection methods using a Schlenk line[12−15] and low temperature colloidal routes.[6,16] In general, for solvothermal and hot injection routes high reaction temperature far above 100 °C, long reaction time (>several hours), and complicated thermal treatment history are needed to form precursor nanoparticles.

The main reason for this is thought to be that most researchers intend to obtain highly crystalline nanoparticles.

On the other hand, it was reported that reaction time of one minute was enough for preparing precursor nanoparticles via the low-temperature colloidal route even without any external heating.[16] Unlike the other preparation methods, the low-temperature colloidal process produced amorphous nanoparticles,[6] which is also expected to have beneficial effects on the postheat treatment. This is because our final goal is not to fabricate highly crystalline nanoparticles, but CIGS thin films with high density. In other words, thermal diffusion of atoms and rearrangement of them into dense film form should be much easier when the starting precursor is in amorphous state rather than in highly crystalline state. It is particularly important because sintering of such highly crystalline CIS nanocrystals is inherently difficult because of the high melting point of CIS, resulting in very limited particle growth and sintering even at high temperature around 500 °C.[17] This has been the most difficult point of the nanoparticle based approaches. In this regard, the low temperature colloidal process is considered to be a very effective particle preparation method on account of not only its fast and simple procedures but also the amorphous products suitable for the post heat treatment.

Fabrication of Cu−In−Ga-Se nanoparticles by the low-temperature colloidal process was first proposed by Schulz in 1998.[6] Therafter, Ahn reported that selenization conditions such the temperature of Se evaporation and the flow rate of

carrier gas significantly affected the growth of the Cu—In—Ga—Se nanoparticles when using their two zone furnace.[5] However, because precise control of Se supply to the precursor films, which was the most important parameter to determine the degree of particle growth, was hard to be achievable with the two zone furnace, results were not reproducible. Regarding conversion efficiencies of the completed solar cells from those amorphous nanoparticles Schulz demonstrated a 4.6% efficient device,[6] but it was achieved only after an additional vacuum evaporation of Ga, In and Se onto the nanoparticle-derived film. Except this, there has been no report of cell efficiency via the amorphous Cu—In—Ga—Se nanoparticle route.

In this regard, the objective of this work is to fabricate device quality CIS thin films from amorphous Cu—In—Se nanoparticles prepared by the low-temperature colloidal route which is a potential low-cost particle synthesis method. We used the Knudsen-type effusion cell as Se evaporation source in order to precisely control the amount of Se vapor supplied to the precursor nanoparticles during selenization. Further, a simple solution-filling technique was introduced to mitigate the electrical short-circuiting in the nanoparticle-derived films, and it resulted in a reproducible cell efficiency of up to 1.98%.

■ EXPERIMENTAL METHODS

Materials. CuI (99.999%), InI$_3$ (99.999%), and Na$_2$Se (99.8%) were purchased from Alfa Aesar; Cu(NO$_3$)$_2$·3H$_2$O (99.999%), InCl$_3$ (99.999%), and pyridine (99.9%) from Sigma Aldrich; methanol (99.6%) and propylene glycol (99%) from Junsei; and elemental Se (99.999%, 3 mm shot) from Cerac.

Synthesis of Precursor Nanoparticles. Basically, we followed the same low-temperature colloidal procedures reported by Schulz[6] and Ahn[16] to produce Cu—In—Se precursor nanoparticles, where a mixture of CuI (0.343 g) and InI$_3$ (0.991 g) in pyridine (30 mL) was reacted with Na$_2$Se (0.5 g) in methanol (20 mL) at 0 °C in an ice bath for 1 min under nitrogen gas atmosphere with mechanical stirring. Because the byproduct of the reaction (NaI) is easily soluble in the methanol while the synthesized Cu—In—Se nanoparticles are insoluble, NaI byproduct could be removed from the product mixture by successive washing and centrifugation with methanol. This resulted in Cu—In—Se nanoparticles forming a stable methanol colloid.

Thin Film Coating. Coating slurry was prepared by adding propylene glycol (PG) as an organic binder to Cu—In—Se/methanol colloids. PG was chosen for its low boiling point (~188 °C), low molecular weight (~79) and appropriate viscosity for doctor blading (40.4 mPa s at 25 °C). The final mixture was stirred with a magnetic bar vigorously for 30 min.

Precursor films were formed by doctor blading (Multi coater, DCN Co. Ltd., Korea) the coating slurry on a 1 μm thick Mo-coated sodalime glass. The samples were then dried at 80 °C for 5 min and then at 180 °C for 2 min in air on a hot plate to evaporate methanol and PG, respectively.

For solution-filling technique, an additional filler solution was prepared by dissolving Cu(NO$_3$)$_2$·3H$_2$O and InCl$_3$ in methanol and adding PG to the solution. Then, this filler solution was coated on the predeposited nanoparticle films by which the filler solution infiltrated into the pores in the underlying films. The same drying treatments as those described above were also applied to the solution-filled samples.

Selenization. Selenization was performed in a vacuum evaporator equipped with a Knudsen-type effusion cell. Initially the chamber was evacuated to a base pressure of 5×10^{-6} Torr with a turbo molecular pump and then elemental Se was evaporated from the effusion cell. Effects of two selenization parameters including a substrate temperature and a Se flux on the growth nature of the precursor particles were investigated. All the samples were selenized for 30 min. The flux of Se vapor was regulated by the effusion cell temperature.

Solar Cell Fabrication. Solar cells were fabricated according to the conventional Mo/CIS/CdS/i-ZnO/n-ZnO/Al structure. A 60 nm thick CdS buffer layer was deposited on CIS film by chemical bath deposition (CBD) and i-ZnO(50 nm)/Al-doped n-ZnO(500 nm) were deposited by radio frequency (rf) magnetron sputtering on the CdS layer. An Al grid of 500 nm in thickness was deposited as a current collector using thermal evaporation. The active area of completed cells was 0.44 cm^2.

Characterization. The morphology, composition, and crystal structure of the nanoparticles, the precursor films, and the selenized films were investigated by the high-resolution scanning electron microscopy (HRSEM, XL30SFEG Phillips Co., Holland at 10 kV), the Energy Dispersive Spectroscopy (EDS, EDAX Genesis apex, acceleration voltage: 30 kV, collection time: 100 s with standard-less method) and the X-ray diffraction (XRD, Rigaku Japan, D/MAX-2500) using CuKα line, respectively. Raman spectra of the nanoparticles were also taken in the quasi-backscattering geometry by using the 514.5 nm line of an Ar ion laser as the excitation source. The scattered light was filtered with a holographic edge filter and dispersed by a Spex 0.55-m spectrometer and detected with a liquid-nitrogen-cooled back-illuminated charge-coupled-device (CCD) detector array. Depth compositional profile of the selenized film was obtained by the Auger electron spectroscopy (AES, Perkin-Elmer, SAM 4300).

Device performances including the conversion efficiency and the EQE (External Quantum Efficiency) were characterized using a class AAA solar simulator (WXS-155S-L2, WACOM, Japan) and an IPCE (Incident Photon Conversion Efficiency) measurement unit (PV measurement, Inc., USA), respectively.

■ RESULTS AND DISCUSSION

Precursor Nanoparticles. We fabricated Cu—In—Se nanoparticles via the low temperature colloidal route as mentioned in the experimental section, in which the starting chemicals reacted for 1 min at 0 °C in an ice bath without any external heating. SEM image of the as-synthesized nanoparticles (Figure 1a) reveals that spherical particles of about 40 nm in diameter with quite uniform size distribution were formed by the reaction. No crystalline peak was detected in XRD pattern of the nanoparticles deposited on Mo/SLG substrate (Figure 1b), demonstrating that the particles shown in Figure 1a are in amorphous state. This is consistent with the results of Schulz[6] and Ahn.[16] The particles were found to have atomic ratio of Cu:In:Se = 0.9:1:2 by EDS measurement (not shown here), which was identical to that of the starting chemicals.

The structure of the particles was further investigated by Raman scattering (Figure 1c). Interestingly, peaks corresponding to In—Se and Cu—Se were detected without any evidence of existence of CuInSe$_2$ ternary phase. This result reveals that our nanoparticles are, in fact, mixtures of amorphous Cu- and In- binary selenides. (This is why we use the notation of Cu—In—Se rather than CuInSe$_2$ when we mention our nanoparticles.)

Besides the potential advantage of the amorphous nature of our particles as precursor materials, the fact that they are mixtures of binary selenides presumably offers another merit. This is particularly due to the existence of Cu—Se with a relatively low melting point of 523 °C. The CuSe phase has been widely used as a liquid flux at the typical CIGS deposition temperature (>500 °C), and has been considered to be responsible for the development of large grains in CIS films formed by vacuum evaporation.[18,19]

In this regard, we claim that the low-temperature colloidal route is an effective low-cost particle preparation method not only for its simple and fast synthesis procedures but also for the structure and phase constitutions of the product particles suitable for the post heat treatment.
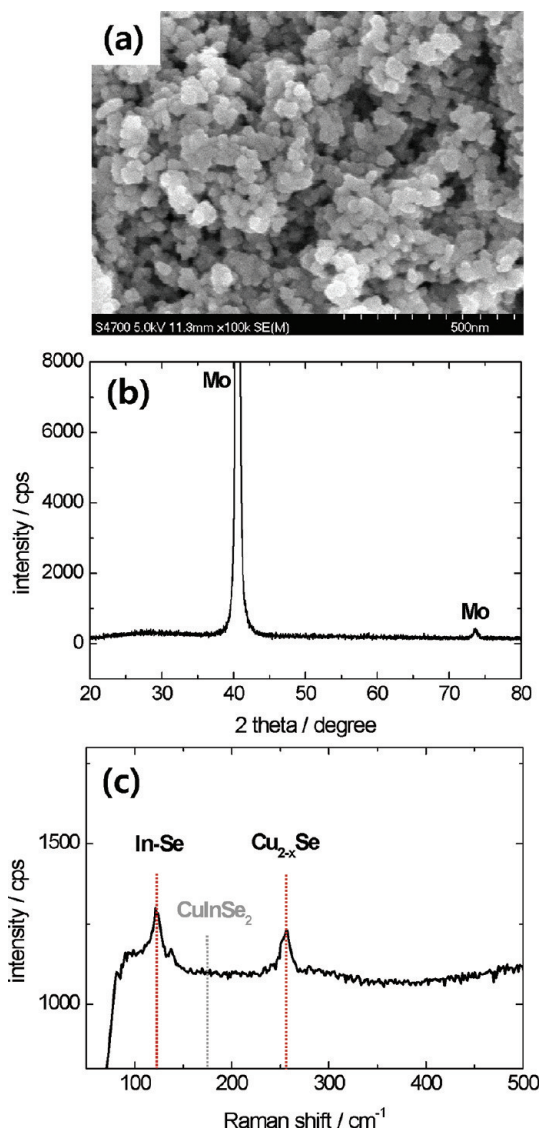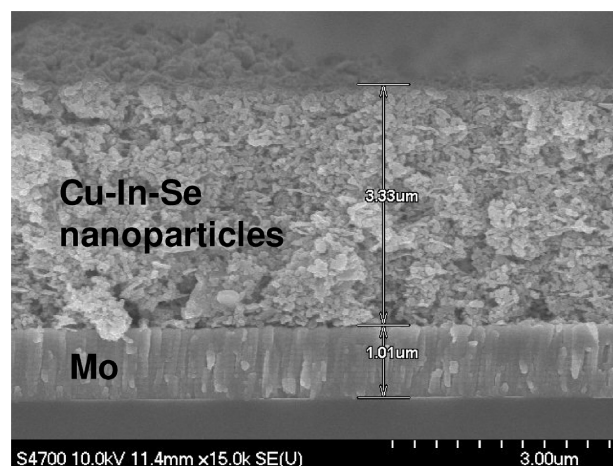
Figure 1. (a) SEM image, (b) XRD pattern, and (c) Raman spectrum of the as-synthesized nanoparticles.

Figure 2. Cross-sectional SEM image of the as-coated film.

Figure 3. XRD patterns of the CIS films selenized at different substrate temperatures.
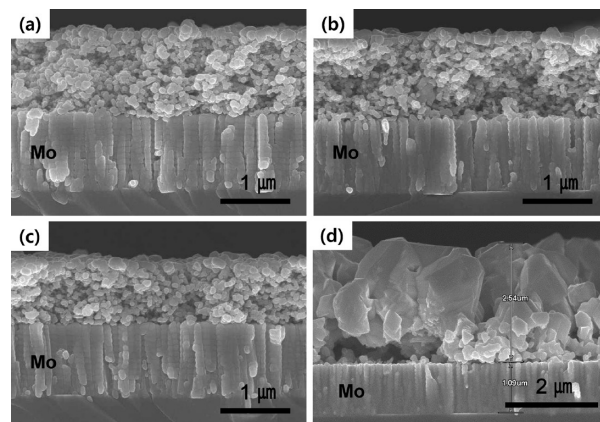
Figure 4. Cross-sectional SEM pictures of the CIS films selenized at different substrate temperatures; (a) 280, (b) 350, (c) 430, and (d) 520 °C.

Effects of Substrate Temperature. A typical cross-sectional SEM image of the as-coated films is shown in Figure 2, where a uniform but porous nanoparticle-based film was formed by the doctor blade coating. Typical thickness of the precursor films was in the range of about 2–3 μm. EDS result revealed that the precursor film had the same chemical composition as those of the particles ($Cu_{0.9}InSe_2$), and carbon was not detected within the detection limit. The latter implies that the organic binder (PG) was effectively evaporated possibly through the pores between particles during the drying process.
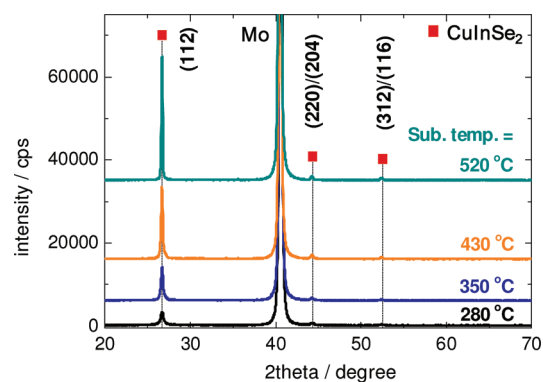
As mentioned in the experimental section, a substrate temperature and a Se flux were chosen as major selenization parameters which primarily determine the growth nature of the nanoparticles.

Figures 3, 4, and 5 show XRD patterns, cross-sectional and plane views of the CIS films selenized at different substrate temperatures, respectively. For this set of experiments, Se flux was fixed to be 10 Å/s.

XRD data (Figure 3) show that all the films have phase pure chalcopyrite structure with strong (112) preferred orientation regardless of the substrate temperature. EDS analysis also revealed that all the films had compositions close to $Cu_{0.9}InSe_2$. From the increase in the peak intensities, crystallinity of the films was found to be improved by increasing substrate temperature.

Regarding the SEM images of the samples, it should be first noted that the thickness of the selenized film is not major information in this study because it significantly depends on the thickness of original as-coated films. Because of the relatively
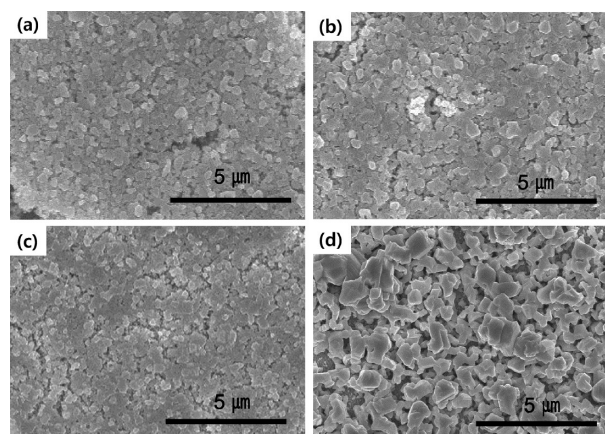
Figure 5. Plane SEM pictures of the CIS films selenized at different substrate temperatures; (a) 280, (b) 350, (c) 430, and (d) 520 °C.

large fluctuation in the thickness of the as-coated films (2−3 μm), only the particle growth nature and corresponding film morphology were analyzed hereafter.

When the precursor nanoparticles were selenized at 280 °C, nonuniform particle growth occurred which is clearly visible in Figure 4a, where the size of particles near the surface region reached about 300 nm and that near Mo back contact was still less than 100 nm. From the fact that particle growth is more pronounced at the surface region where the Se vapor is supplied to meet the particles it can be inferred that Se vapor plays a great role in the particle growth, which is consistent with the reports from Ahn.[5,7]

The features of particle growth by selenization were not noticeably changed until the substrate temperature increased up to 430 °C. However, an abrupt change in growth nature of the particles were observed when the selenization was performed at 520 °C (Figure 4d), in which significant particle growth occurred and the final particle size reached the film thickness (>2 μm). This facile particle growth has rarely been reported primarily because sintering of highly crystalline CIGS nanoparticles is difficult because of the high melting point of CIGS.[17,20] Interestingly, this substrate temperature of 520 °C (Figure 4d) is very close to the melting temperature of CuSe binary phase, which was found to exist in our binary mixture precursors. From this result, we claim that the significant growth of the Cu−In−Se nanoparticles by selenization at 520 °C is closely related to the presence of amorphous Cu−Se phase in the precursor particles, also supported by the fact that

particle growth was not remarkable when the substrate temperature was in the range of 280 to 430 °C. These growth features confirms again that our amorphous binary mixture nanoparticles have large potential in terms of their facile growth by selenization.

However, closely looking at the surface morphology of the film selenized at 520 °C (Figure 5d), one can see that the particle growth occurred according to the Ostwald ripening in which larger particles grew by continuously drawing and consuming materials from smaller ones. This left even larger voids in the final film compared to those in the as-coated film, which is opposite to the original intention of performing selenization. We fabricated solar cells using the CIS films shown in Figures 4 and 5, but they did not show any photoresponse and in the dark I−V measurements all the devices showed complete short-circuiting (linear I−V characteristics) regardless of the substrate temperature. This can be attributed to the direct contacting of the buffer and TCO materials with Mo layer thorough the voids in the CIS films.

Accordingly, as a next step, we performed following two sets of experiments with a main intention to decrease the porosity of the final films.

Control of Se Flux. Investigation into effects of Se flux on the growth nature of the particles is based on an idea that amount of the liquid phase should have great influence on the liquid assisted sintering behavior. In our case, we intended to control the amount of liquid Cu−Se phase by changing Se flux during selenization. This is also motivated by the report of Kim[21] in which the authors stated that the relative amount of Cu−Se liquid phase during the 3-stage coevaporation process significantly depended on the Se flux. Using Cu−Se phase diagram they suggested that the higher the Se flux, the larger the amount of liquid phase. This resulted in an enhanced long-range and fast diffusion, leading to a facile but too rapid growth of the grains. They also claimed that the rapid grain growth was the main reason for the pit and pore formation in the film grown under high Se flux condition.[21]

Figure 6 shows the SEM images of the films selenized under different Se flux conditions. All the samples were selenized at 520 °C. Apparently, increase in Se flux from 10 to 50 Å/s had no influence on particle growth and corresponding film morphologies, implying that Se flux of 10 Å/s was already high enough and further Se supply might simply induce re-evaporation of Se vapor. However, decrease of Se flux down to 5 Å/s resulted in a noticeable suppression of particles growth, reflecting that Se flux of 5 Å/s was insufficient to liquidize all
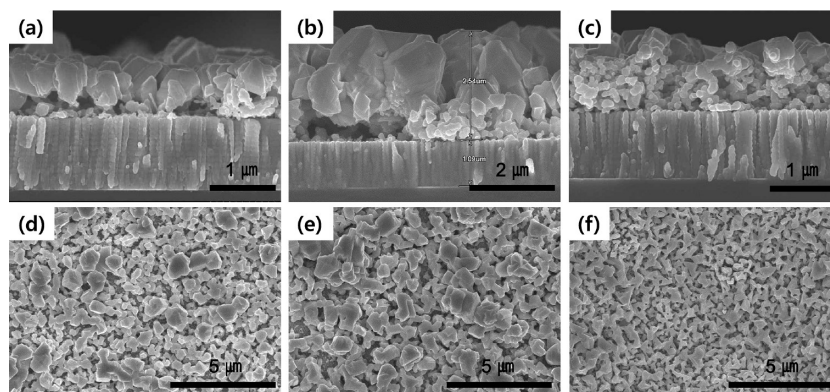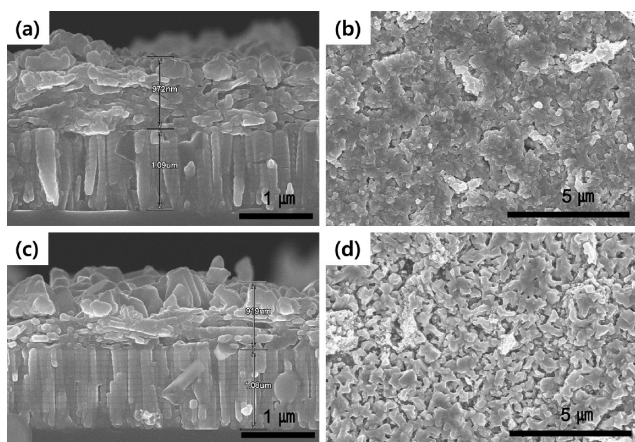

Figure 6. SEM images of the CIS films selenized under different Se flux conditions; (a, d) 50, (b, e) 10, and (c, f) 5 Å/s.

the Cu−Se binaries present in the film. In this case, particle growth occurred only at the surface region (Figure 6c), confirming again that Se vapor played a critical role in the particle growth presumably by determining the amount of Cu−Se liquid phase.

However, even in the case of low Se flux of 5 Å/s, growth mode of the particles and the corresponding film morphologies were not much improved. These results mean that although our amorphous binary mixture nanoparticles have advantage in terms of their facile growth, the growth behavior is not desirable for film densification at this stage.

Solution Filling. The second strategy for reducing the porosity of the final films is applying a solution-filling step to the nanoparticle derived films. This approach is based on another simple idea that we may adjust the porosity of the as-coated film itself as low as possible by filling the pores with source materials such as Cu and In. In this way, it is expected to obtain more densely packed precursor films and also the final films with higher density. These films are designated as "solution-filled films" to be differentiated from the "particle only films" mentioned in the previous sections.

Figure 7 shows SEM micrographs of the solution-filled films selenized at different substrate temperatures. Se flux was fixed
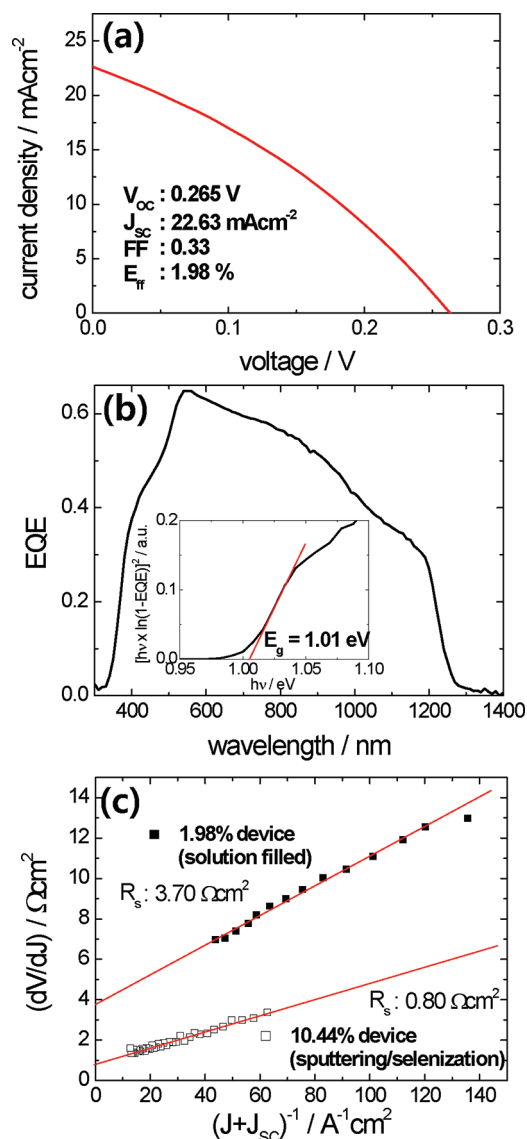
Figure 7. SEM images of the solution-filled films selenized at different substrate temperatures; (a, b) 430 and (c, d) 520 °C.

to be 10 Å/s. In general, dependency of the film morphologies on the substrate temperature was similar to those shown in Figure 4 in that the higher the temperature, the rougher the film. However, the cross-sectional images clearly show that porosity of the films is significantly reduced by the solution-filling treatment.

We fabricated solar cells using both the films and they demonstrated conversion efficiencies of 1.98% (for the film selenized at 430 °C) and 0.9% (at 520 °C), respectively. The lower efficiency at higher temperature can be attributed to the rougher surface morphology, meaning the larger number of short-circuiting paths. However, compared to the fully short-circuited cases for the "particle only films", these results show that the solution-filling treatment is effective in mitigating the direct contact between TCO and back contact.

Characteristics of the 1.98% device are presented in Figure 8. External quantum efficiency (EQE) data (Figure 8(b)) exhibited a long end tail with a gradually decreasing EQE from about 570 nm, which is attributed to a short minority carrier lifetime. Bandgap of the CIS layer was estimated from

Figure 8. Characteristics of the CIS solar cell fabricated with the "solution-filled film" selenized at 430 °C; (a) I−V curve measured under AM 1.5G condition, (b) EQE curve and E_g value (inset), and (c) R−J curve redrawn from a. For comparison, an R−J curve of a CIS solar cell with conversion efficiency of 10.44% prepared by a sputtering/selenization process is presented in c.

the $[h\nu\ln(1 - EQE)]^2$ against $h\nu$ relationship (inset in Figure 8b), showing a value of 1.01 eV, which is consistent with previously reports.[22,23] Figure 8a was further converted to dJ/dV vs V and R−J forms to extract shunt conductance (G) and series resistance (R_S), respectively. These values are compared to those of a 10.44% CIS solar cell fabricated by a sputtering/selenization technique in our laboratory.

From dJ/dV vs V relation (not shown here), G was measured to be around ∼40 mS cm^{-2}. This value is high compared to that of the 10.44% device (∼10 mS cm^{-2}). The R−J curve presented in Figure 8c also demonstrates that the 1.98% device suffers from much higher R_S compared to the 10.44% CIS device.

To elucidate the reasons for the inferior device performance, we performed AES analysis on the solution-filled CIS film selenized at 430 °C (Figure 9a). Depth profile reveals that there is significant amount of residual carbons (up to ∼25 at %) throughout the entire film. Compared to the nearly carbon-free
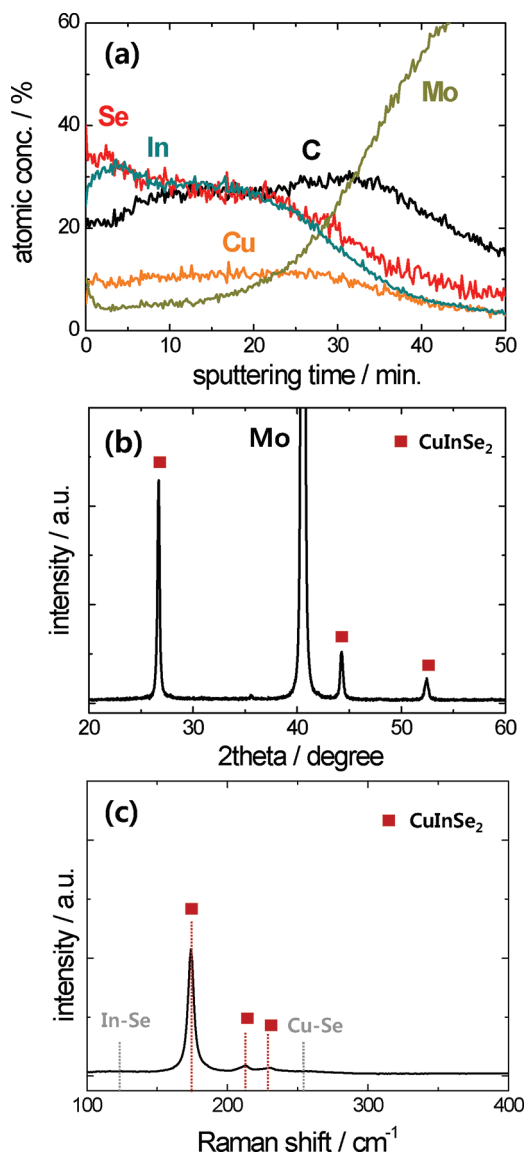
Figure 9. (a) AES depth profile, (b) XRD pattern, and (c) Raman spectrum of the solution-filled CIS film selenized at 430 °C.

"particle only" films (Figures 2, 4, 5, and 6), it is certain that these carbons came from the filler solution. It means that even though the same binder, PG, was used both for the particle coating and the additional solution coating, its evaporating nature is critically influenced by what the deposited materials are. It was already mentioned that PG was almost completely removed when we coated the nanoparticles, presumably through the pores between the particles. We dried the "particle only" samples at 180 °C for 2 min in air, but in fact the evaporation of PG and corresponding drying nature of the films were not significantly affected by temperature within a range of 150 to 300 °C. On the other hand, in the solution coating process, the morphologies of the dried film was critically influenced by the drying temperature. For example, we could not increase the temperature over 180 °C because further temperature increase induced a significant blistering of the sample. This reflects that there might be a blocking layer at the sample surface (possibly a CuCl crystalline layer) preventing facile evaporation of PG. As a result, we kept the drying temperature of the solution-filled precursor film lower than 180

°C and this might be the main reason for the high carbon content in the AES profile. This blocking layer related hypothesis is partially supported by the previous paper which reported that drying of a film deposited by using Cu-nitrate and In-chloride as starting chemicals and ethyl-cellulose as an organic binder resulted in a formation of CuCl crystals, and finally it led to a formation of double layered structure with upper CIS layer and bottom carbon residue layer.[23]

Another interesting point is that the preferred orientation of the selenized film was influenced by the solution-filling treatment. Comparing XRD pattern of the "particle only" film selenized at 430 °C (Figure 3) with that of the "solution-filled" film selenized at the same temperature (Figure 9b), it is clear that the former shows a much higher (112)/(220) intensity ratio. It is well-established that in a Cu-poor CIS chacolpyrite structure polar (112) planes stabilized by Cu vacancies are more stable than the nonpolar (220) planes.[24] Thus, if there is enough time and activation energy, i.e., substrate temperature, for atoms to find place in existing crystals during the film growth process, newly forming crystals are expected to grow along the (112) planes. On the other hand, if the atoms is just condensed or should start new crystal growth the resulting films might lose their (112) preferred orientation. In our case, the crystal growth reaction starts from the film surface exposed to Se vapor. For the "particle only" film, underlying particles should easily find low energy planes of the existing crystals and it presumably results in a strong (112) texture as presented in Figure 3. However, for the "solution-filled" film there are large amount of carbon impurities as clearly shown in the AES depth profile (Figure 9a) which force the underlying particles to grow more randomly, resulting in reduced (112) texture.

Apart from the carbon residue, the Cu:In:Se ratio of the film (close to 10:25:25) is far from the stoichiometry (1:1:2). XRD (Figure 9b) and Raman spectrum (Figure 9c) of the sample reveal that the only crystalline phase is α-CuInSe$_2$, thus the solution-filled film should be considered as a mixture of α-CuInSe$_2$ and low crystalline In-compounds embedded in carbon.

Accordingly, the high G and R_S values of the 1.98% device should be attributed to the compositional imperfections of the CIS film and the high carbon content, which are certainly originated from the PG/methanol solution containing Cu and In ions.

From these experimental results, it was revealed that in the amorphous Cu–In–Se nanoparticle based route the main technical issue is not the particle growth, which has long been the most important issue in the highly crystalline nanoparticle based routes, but the control of the nonuniform growth nature of the particles. Further compositional optimization is expected to improve the device performance significantly, in which the main topic will be an application of different organic additives rather than PG in the filler solution which leave less amount of carbon residue and suppress the nonuniform growth of particles even at high temperature of over 500 °C to fully utilize the advantages of our amorphous Cu–In–Se nano-particles.

■ CONCLUSIONS

CuInSe$_2$ (CIS) absorber layers for thin film solar cells were fabricated via a nonvacuum route using nanoparticle precursors. By a low-temperature colloidal process, amorphous binary mixture (Cu–Se and In–Se) nanoparticles were formed within 1 min of reaction without any external heating, reflecting the

potential of this process as a low-cost particle preparation method. Selenization of the nanoparticle coated film resulted in a facile growth of the particles up to micrometer scale. However, selenization resulted in a nonuniform growth of the particles' remaining large voids in the final films, which acted as short circuiting paths in corresponding solar cells. To overcome this problem, we applied an additional solution-filling treatment to the precursor film by which a solution containing Cu and In ions infiltrated into the pores in the precoated nanoparticles. This approach resulted in a mitigation of the short circuiting of the device, and a conversion efficiency of up to 1.98% from a CIS film selenized at 430 °C. This is the first report on a working device prepared from amorphous Cu−In−Se nanoparticles synthesized in a facile and simple manner.

■ AUTHOR INFORMATION

Corresponding Author

*Tel: +82-42-860-3199. Fax: +82-42-860-3739. E-mail: y-kh@ kier.re.kr.

Notes

The authors declare no competing financial interest.

■ ACKNOWLEDGMENTS

■ REFERENCES

(1) Repins, I.; Contreras, M. A.; Egaas, B.; DeHart, C.; Scharf, J.; Perkins, C. L.; To, B.; Noufi, R. *Prog. Photovolt: Res. Appl.* **2008**, *16*, 235.

(2) Green, M. A.; Emery, K.; Hishikawa, Y.; Warta, W. *Prog. Photovolt.: Res. Appl.* **2011**, *19*, 84.

(3) Eberspacher, C.; Fredric, C.; Pauls, K.; Serra, J. *Thin Solid Films* **2001**, *387*, 18.

(4) Weil, B. D.; Connor, S. T.; Cui, Y. *J. Am. Chem. Soc.* **2010**, *132*, 6642.

(5) Ahn, S. J.; Kim, K. H.; Yun, J. H.; Yoon, K. H. *J. Appl. Phys.* **2009**, *105*, 113533.

(6) Schulz, D. L.; Curtis, C. J.; Flitton, R. A.; Weisner, H.; Keane, J.; Matson, R. J.; Jones, K. M.; Parilla, P. A.; Noufi, R.; Ginley, D. S. *J. Electron. Mater.* **1998**, *27*, 433.

(7) Ahn, S. J.; Kim, C. W.; Yun, J. H.; Lee, J. C.; Yoon, K. H. *Sol. Energy Mater. Sol. Cells* **2007**, *91*, 1836.

(8) Chun, Y. G.; Kim, K. H.; Yoon, K. H. *Thin Solid Films* **2005**, *480−481*, 46.

(9) Yu, C.; Yu, J. C.; Wen, H.; Zhang, C. *Mater. Lett.* **2009**, *63*, 1984.

(10) Jiang, Y.; Wu, Y.; Mo, X.; Yu, W. C.; Xie, Y.; Qian, Y. T. *Inorg. Chem.* **2000**, *39*, 2964.

(11) Lu, Q. Y.; Hu, J. Q.; Tang, K. B.; Qian, Y. T.; Zhou, G. E.; Liu, X. M. *Inorg. Chem.* **2000**, *39*, 1606.

(12) Tang, J.; Hinds, S.; Kelly, S. O.; Sargent, E. H. *Chem. Mater.* **2008**, *20*, 6906.

(13) Panthani, M. G.; Akhavan, V.; Goodfellow, B.; Schmidtke, J. P.; Dunn, L.; Dodabalapur, A.; Barbara, P.; Korgel, B. A. *J. Am. Chem. Soc.* **2008**, *130*, 16770.

(14) Guo, Q.; Kim, S. J.; Kar, Shafarman, W. N.; Birkmire, R. W.; Stach, E. A.; Agrawal, R.; Hillhouse, H. W. *Nano Lett.* **2008**, *8*, 2982.

(15) Guo, Q.; Ford, G. M.; Hilllhouse, H. W.; Agrawal, R. *Nano Lett.* **2009**, *9*, 3060.

(16) Ahn, S. J.; Kim, K. H.; Chun, Y. G.; Yoon, K. H. *Thin Solid Films* **2007**, *515*, 4036.

(17) Hibberd, C. J.; Chassaing, E.; Liu, W.; Mitzi, D. B.; Lincot, D.; Tiwari, A. N. *Prog. Photovolt: Res. Appl.* **2009**, *18*, 434.

(18) Klenk, R.; Walter, T.; Schock, H. W.; Cahen, D. *Adv. Mater.* **1993**, *5*, 114.

(19) Tuttle, J. R.; Contreras, M.; Bode, M. H.; Niles, D.; Albin, D. S.; Matson, R.; Gabor, A. M.; Tennant, A.; Duda., A.; Noufi, R. *J. Appl. Phys.* **1995**, *77*, 153.

(20) Arita, T.; Suyama, N.; Kita, Y.; Kitamura, S.; Hibino, T.; Takada, H.; Omura, K.; Ueno, N.; Murozono, M. CuInSe$_2$ films prepared by screen-printing and sintering method. In *Conference Record of the Twentieth IEEE Photovoltaic Specialists Conference*; Las Vegas; IEEE: Piscataway, NJ, 1988; p 1650.

(21) Kim, K. H.; Yoon, K. H.; Yun, J. H.; Ahn, B. T. *Electrochem. Solid-State Lett.* **2006**, *9*, A382.

(22) Chichibu, S.; Mizutani, T.; Murakami, K.; Shioda, T.; Kurafuji, T.; Nakanish, H.; Niki, S.; Fons, P. J.; Yamada, A. *J. Appl. Phys.* **1998**, *83*, 3678.

(23) Ahn, S. J.; Kim, C. W.; Yun, J. H.; Gwak, J.; Jeong, S.; Ryu, B. H.; Yoon, K. H. *J. Phys. Chem. C* **2010**, *114*, 8108.

(24) Jaffe, J. E.; Zunger, A. *Phys. Rev. B* **2001**, *64*, 241304.